THE JOURNAL OF BIOLOGICAL CHEMISTRY
Vol. 276, No. 39, Issue of September 28, pp. 36606–36612, 2001

Printed in U.S.A.

Mapping the Interacting Regions between Troponins T and C

BINDING OF TnT AND TnI PEPTIDES TO TnC AND NMR MAPPING OF THE TnT-BINDING SITE ON TnC*

Received for publication, June 5, 2001, and in revised form, July 24, 2001
Published, JBC Papers in Press, July 25, 2001, DOI 10.1074/jbc.M105130200

Tharin M. A. Blumenschein, Brian P. Tripet, Robert S. Hodges, and Brian D. Sykes‡

From the Canadian Institutes of Health Research Group in Protein Structure and Function, Department of Biochemistry, University of Alberta, Edmonton, Alberta T6E 1X9, Canada

Muscular contraction is triggered by an increase in calcium concentration, which is transmitted to the contractile proteins by the troponin complex. The interactions among the components of the troponin complex (troponins T, C, and I) are essential to understanding the regulation of muscle contraction. While the structure of TnC is well known, and a model for the binary TnC·TnI complex has been recently published (Tung, C.-S., Wall, M. E., Gallagher, S. C., and Trewhella, J. (2000) *Protein Sci.* 9, 1312–1326), very little is known about TnT. Using non-denaturing gels and NMR spectroscopy, we have analyzed the interactions between TnC and five peptides from TnT as well as how three TnI peptides affect these interactions. Rabbit fast skeletal muscle peptide TnT-(160–193) binds to TnC with a dissociation constant of 30 ± 6 μM. This binding still occurs in the presence of TnI-(1–40) but is prevented by the presence of TnI-(56–115) or TnI-(96–139), both containing the primary inhibitory region of TnI. TnT-(228–260) also binds TnC. The binding site for TnT-(160–193) is located on the C-terminal domain of TnC and was mapped to the surface of TnC using NMR chemical shift mapping techniques. In the context of the model for the TnC·TnI complex, we discuss the interactions between TnT and the other troponin subunits.

Skeletal muscle contraction is regulated by troponin and tropomyosin located in the thin filament. Contraction begins with the binding of Ca^{2+} to the troponin complex, triggering conformational changes that are propagated to tropomyosin and actin. The troponin complex is constituted by a Ca^{2+}-binding subunit, troponin C (TnC),[1] an inhibitory subunit, troponin I (TnI), and a tropomyosin-binding subunit, troponin T (TnT). When the muscle is relaxed, TnI inhibits myosin ATPase activity. The smallest region of TnI capable of this inhibition is known as the inhibitory region, or the inhibitory peptide (residues 96–115). Upon binding of Ca^{2+}, TnC undergoes conformational changes and removes the inhibition by TnI. TnT binds to TnI, TnC, and tropomyosin, anchoring the troponin complex to the thin filament and propagating the conformational changes (for reviews, see Refs. 1–3). The interactions among the three components in the troponin complex as well as how they are affected by the presence of calcium are essential for understanding the regulation of muscle contraction.

The structure of skeletal TnC is well known and has been determined by both x-ray crystallography (4–6) and nuclear magnetic resonance (NMR) spectroscopy (7). NMR and crystallographic data provided some structural information on the interaction between TnC and fragments of TnI (8–14). A model for the structure of the skeletal binary TnC·TnI complex was recently built based on a number of binding and activity assays such as cross-linking, fluorescent resonance energy transfer (FRET), and neutron scattering data as well as the available structural information (15).

Despite the amount of information on the interactions between TnC and TnI that has emerged in the last few years, not much is known about the structure of TnT, either isolated or interacting with another troponin subunit. Rabbit skeletal TnT yields two fragments when digested by chymotrypsin. The N-terminal fragment, known as T1, binds to tropomyosin, while the C-terminal fragment, T2, binds TnI and TnC (for reviews, see Refs. 3 and 16). Although TnI by itself inhibits myosin ATPase and TnC can remove the inhibition, TnT is necessary for the Ca^{2+}-dependent regulation of myosin ATPase by the troponin complex. Direct interaction of TnT with TnC is responsible for this calcium-sensitizing effect (17).

Herein we show that two TnT peptides, containing residues 160–193 and 228–260, bind to TnC and that other peptides in the T2 region do not bind TnC. We also show that two TnI peptides containing the inhibitory region compete with TnT-(160–193) for TnC, while the first 40 residues of TnI bind to TnC simultaneously with TnT-(160–193). Using two-dimensional ^{1}H,^{15}N NMR spectroscopy to follow the titration of TnC with the peptide TnT-(160–193), we calculated the binding constant for this peptide and mapped the binding region on the surface of TnC. We show this mapping on the model of the binary TnC·TnI complex and discuss the competition results in this context.

MATERIALS AND METHODS

Proteins and Peptides—The expression and purification of recombinant chicken skeletal TnC, NTnC, CTnC, [^{15}N]TnC, and [^{13}C,^{15}N]CTnC were performed as described previously (14, 18, 19). The rabbit fast skeletal muscle TnI and TnT peptide analogs were synthesized by solid phase peptide synthesis methodology and purified by reverse phase high performance liquid chromatography, as described (20–23). TnT residue numbers correspond to isoform TnT_{2f} (24). The peptide sequences were: TnT-(151–170), acetyl-SMGANYSSYLAKADQKRGKK-NH_2; TnT-(160–193), acetyl-LAKADQKRGKKQTAREMKKKILAER-RKPLNIDHL-NH_2; TnT-(181–215), acetyl-LAERRKPLNIDHLSDEK-LRDKAKELWDTLYQLETD-NH_2; TnT-(209–243), acetyl-LYQLETDK-FEFGEKLKRQKYDIMNVRARVEMLAKF-NH_2; TnT-(228–260), acetyl-YDIMNVRARVEMLAKFSKKAGTTAKGKVGGRWK-NH_2; TnI-(1–40), acetyl-GDEEKRNRAITARRQHLKSVMLQIAATELEKEEG-

* This work was supported by the Canadian Institutes of Health Research. The costs of publication of this article were defrayed in part by the payment of page charges. This article must therefore be hereby marked "*advertisement*" in accordance with 18 U.S.C. Section 1734 solely to indicate this fact.

‡ To whom correspondence should be addressed. Tel.: 780-492-5460; Fax: 780-492-0886; E-mail: brian.sykes@ualberta.ca.

[1] The abbreviations used are: TnC, troponin C; TnI, troponin I; TnT, troponin T; CTnC, C domain (residues 88–162) of recombinant chicken skeletal troponin C; NTnC, N domain (residues 1–90) of recombinant chicken skeletal troponin C; HSQC, heteronuclear single-quantum coherence.

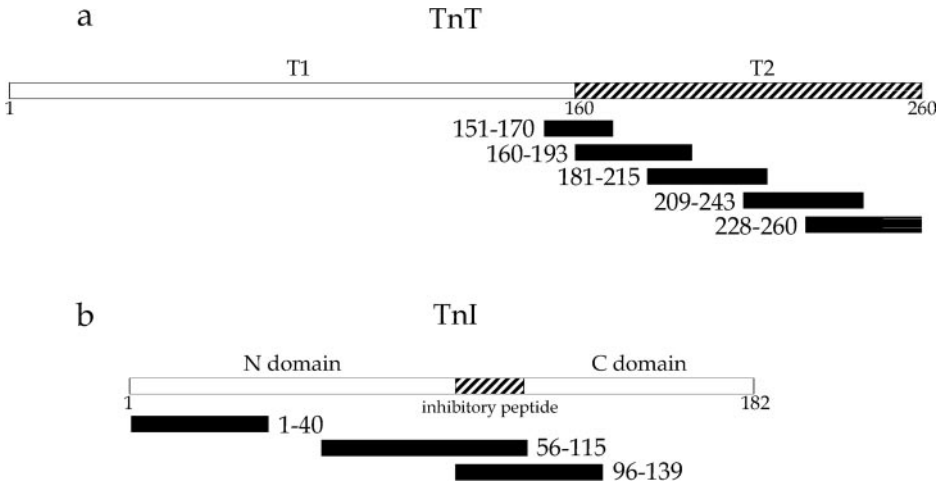

FIG. 1. **Schematic representation of the peptides used in this work.** *a*, five TnT peptides spanning the whole T2 region; *b,* three TnI peptides used for competition assays with the TnT peptides. The sequence of the peptides is described under "Materials and Methods."

RREAEK-NH_2; TnI-(56–115), acetyl-SMAEVQELCKQLHAKIDAA-EEEKYDMEIKVQKSSKELEDMNQKLFDLRGKFKRPPLRRVR-NH_2; TnI-(96–139), acetyl-NQKLFDLRGKFKRPPLRRVRMSADAMLKA-LLGSKHKVCMDLRAN-NH_2. Proteins and peptides were lyophilized and resuspended in NMR buffer or non-denaturing gel electrophoresis buffer in appropriate concentrations. All protein and peptide concentrations were determined by amino acid analysis in duplicate.

Gel Electrophoresis—TnC complexes with TnT and TnI peptides were visualized on 10% glycerol-polyacrylamide gels (25). Unlabeled recombinant TnC (or the individual domains) and the peptides were resuspended in 20 mM Hepes pH 7.6, 100 mM NaCl, and 5 mM $CaCl_2$. TnT-(209–243) could not be resuspended in the buffer and was resuspended directly in TnC solution. Protein concentrations were determined to be 25 μM for TnC, 19 μM for CTnC, 16 μM for NTnC, 143 μM for TnT-(151–170), 104 μM for TnT-(160–193), 59 μM for TnT-(181–215), 128 μM for TnT-(209–243), 185 μM for TnT-(228–260), 89 μM for TnI-(1–40), 103 μM for TnI-(56–115), and 186 μM for TnI-(96–139). TnC and TnT or TnI peptides were mixed in ratios from 1:1 to 1:4. TnC/TnI/TnT mixtures were made in 1:1:1 ratios. The mixtures were incubated for at least 30 min at room temperature before analysis and then diluted in sample buffer and analyzed in 10% glycerol, 8% polyacrylamide gels as described (26).

TnT-(160–193) Titration of [^{15}N]TnC—Recombinant TnC uniformly labeled with ^{15}N and the peptide TnT-(160–193) were resuspended in 100 mM KCl, 10 mM imidazole, 20 mM dithiothreitol, 6 mM $CaCl_2$, 0.03% sodium azide, and 0.2 mM 2,2-dimethyl-2-silapentane-5-sulfonic acid in 90% H_2O, 10% D_2O at pH 6.9. TnC concentration in the initial NMR sample was 0.6 mM, and TnT-(160–193) concentration in the stock solutions was 21 and 62 mM, respectively. Titration points of 0.14, 0.29, 0.43, 0.57, 0.71, 0.86, 1, 1.14, 1.29, 1.43, 1.87, and 2.3 molar equivalents of TnT-(160–193) were observed consecutively. 2-μl aliquots of the 21 mM solution were added for the first 10 points, and 2-μl aliquots of the 62 mM solution were added for the last two points. Both one-dimensional ^{1}H and two-dimensional ^{1}H,^{15}N HSQC NMR spectra were acquired at every titration point.

TnT-(160–193) Titration of [^{13}C,^{15}N]CTnC—Recombinant CTnC uniformly labeled with ^{15}N and ^{13}C and the peptide TnT-(160–193) were resuspended in 100 mM KCl, 10 mM imidazole, 20 mM dithiothreitol, 6 mM $CaCl_2$, 0.03% sodium azide, and 0.2 mM 2,2-dimethyl-2-silapentane-5-sulfonic acid in 90% H_2O, 10% D_2O at pH 6.9. CTnC concentration in the initial NMR sample was 0.9 mM, and TnT-(160–193) concentration in the stock solution was 33 mM. Titration points of 0.15, 0.30, 0.44, 0.59, 0.74, 0.89, 1.03, 1.18, 1.33, and 1.48 molar equivalents of TnT-(160–193) were observed consecutively. 2-μl aliquots of the stock solution were added for each point. Both one-dimensional ^{1}H and two-dimensional ^{1}H,^{15}N HSQC NMR spectra were acquired at every titration point. A last point was acquired later, with 0.54 mM CTnC and 4.69 molar equivalents of TnT-(160–193).

NMR Spectroscopy—All one-dimensional ^{1}H and two-dimensional ^{1}H,^{15}N HSQC NMR spectra were acquired on a Varian Unity 600 MHz spectrometer. One-dimensional ^{1}H spectra were acquired using spectral widths of 7500 or 8000 Hz, a ^{1}H pulse width of 10 μs (90°), and an acquisition time of 2 s. The ^{1}H,^{15}N HSQC NMR spectra were acquired using the sensitivity-enhanced gradient pulse sequence developed by Lewis E. Kay and co-workers (27, 28). ^{1}H and ^{15}N sweep widths were 8000 and 1650 Hz, respectively. 24 transients were acquired for each titration point. The data sets were processed using the VNMR software package (VNMR 6.1B Varian, Palo Alto, CA) and the programs NMRPipe (29) and NMRView (30).

RESULTS

Non-denaturing Gel Electrophoresis—The five TnT peptides shown in Fig. 1*a* (TnT-(151–170), TnT-(160–193), TnT-(181–215), TnT-(209–243), and TnT-(228–260)) were individually mixed with TnC in the presence of Ca^{2+} and applied to a non-denaturing gel. TnT-(160–193) and TnT-(228–260) are able to displace the TnC band, thus binding to TnC (Fig. 2*a*). Therefore, TnT-(160–193) and TnT-(228–260) contain the probable sites in TnT responsible for the interaction with TnC. However, when TnT-(228–260) is mixed with TnC in TnC/TnT-(228–260) ratios larger than 1:3, the TnC band cannot be seen in the gel (data not shown). This probably results from the nonspecific binding of multiple copies of TnT-(228–260) to TnC. For this reason, this study focuses on the interactions between TnT-(160–193) and TnC. TnT-(181–215) can be seen as a separate band in the gel in the presence or absence of TnC because of its negative charge and does not affect the TnC band. In the absence of Ca^{2+} (1 mM EGTA, 10 mM $MgCl_2$), none of the peptides bound TnC (data not shown).

When the TnC-binding peptide TnT-(160–193) is mixed to the individual domains of TnC in the presence of Ca^{2+}, it causes a partial displacement of the C domain (CTnC) band (Fig. 2*b*) but not of the N domain (NTnC) band. This suggests that the interaction between TnT-(160–193) and TnC occurs through the C domain of the protein. The weakening of the NTnC band suggests some binding to the N domain, but no band for the complex is seen. Given the charges of NTnC and TnT-(160–193), a stable complex should be seen in the gel. A weak complex would dissociate while migrating in the gel and would not be seen as a band.

TnI peptides described in Fig. 1*b* (TnI-(1–40), TnI-(56–115), and TnI-(96–169)) were combined with TnC and TnT-(160–193) to evaluate how they would affect the interaction between TnC and TnT-(160–193). TnT-(160–193) and the peptide containing the first 40 amino acids from TnI (TnI-(1–40)) can bind to TnC simultaneously. When either of the two peptides is added to TnC, the TnC band is displaced. When both peptides are added to TnC, the resulting displacement is bigger, roughly corresponding to the sum of both individual displacements (Fig. 2*c*). This displacement shows the simultaneous binding of the two peptides to TnC. TnT-(160–193) binds to TnC with smaller affinity than TnI-(1–40), causing only a partial displacement when mixed to TnC, whereas TnI-(1–40) displaces the band totally. When the two peptides are added simultaneously to TnC, some of the TnC·TnI-(1–40) band is still seen because of the weaker binding of TnT-(160–193).

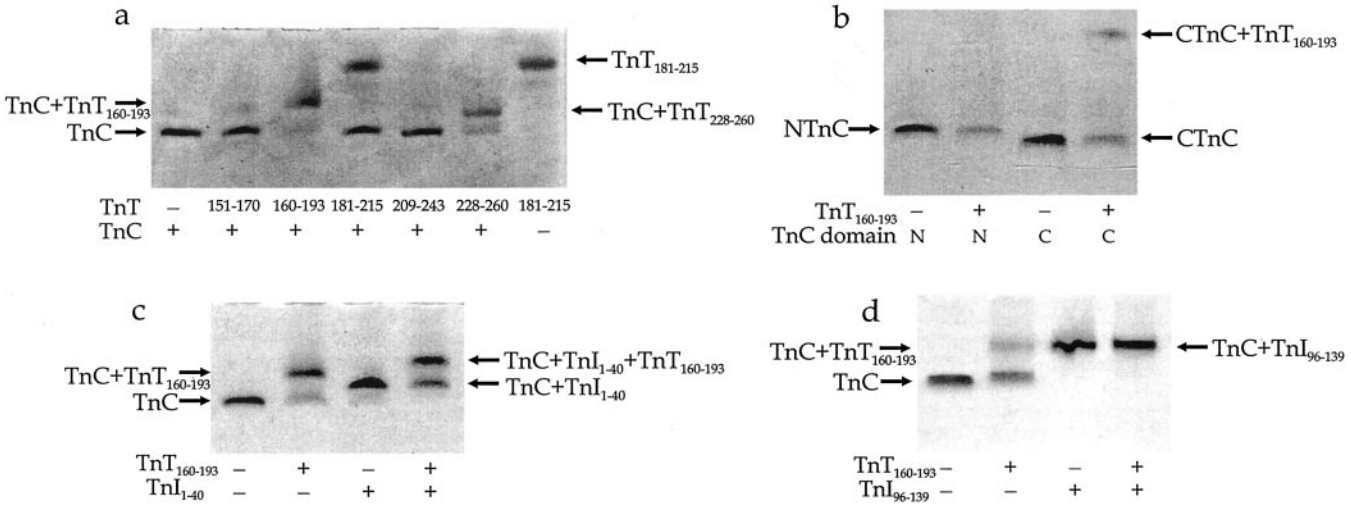

FIG. 2. **Interaction between TnC (whole protein or individual N or C domains) and TnT and TnI peptides.** TnC was combined with one or two peptides at a time, as described under "Material and Methods," and the mixture was analyzed by non-denaturing gel electrophoresis. Specific combinations of peptides and/or proteins are indicated at the *bottom* of the gels. Gels *c* and *d* contain TnC in all *lanes*. *a*, each of the five TnT peptides was mixed with TnC. TnT-(160–193) and TnT-(228–260) displace the TnC band and therefore bind to TnC. The TnC/peptide ratio was 1:4 for all the peptides except TnT-(228–260). The TnC/TnT-(228–260) ratio was 1:3. *b*, TnT-(160–193) mixed with the individual domains of TnC. TnT-(160–193) caused a displacement of the CTnC band but not the NTnC band. The TnC/peptide ratio was 1:4. *c*, TnT-(160–193) and TnI-(1–40) bind simultaneously to TnC, causing a double displacement of the TnC band. The ratio used in this gel was 1:1:1 (TnC/TnI-(1–40)/TnT-(160–193)). *d*, TnT-(160–193) and TnI-(96–139) compete for TnC. When both peptides are added to TnC the only band displacement seen is the one caused by TnI-(96–139). The ratio in this gel was 1:1:1 (TnC/TnI-(96–139)/TnT-(160–193)).

When TnI-(96–139) is combined with TnC and TnT-(160–193), a different result is obtained. The only displacement seen on the TnC band is the one caused by the binding of TnI-(96–139) (Fig. 2*d*), which binds to TnC with greater affinity than TnT-(160–193) and prevents it from binding. The greater affinity of TnI-(96–139) can be seen from the complete displacement of the TnC band that it causes, whereas TnT-(160–193) only produces partial displacement.

The same experiment was done with TnI-(56–115) and TnT-(160–193). As with TnI-(96–139), TnI-(56–115) also competes with TnT-(160–193), preventing it from binding TnC (data not shown).

Titration of [^{15}N]TnC and [^{13}C,^{15}N]CTnC with TnT-(160–193)—TnT-(160–193) was titrated into [^{15}N]TnC and [^{13}C,^{15}N]CTnC solutions. The binding was followed by two-dimensional ^{1}H,^{15}N HSQC NMR spectroscopy. The two-dimensional ^{1}H,^{15}N HSQC NMR spectra of [^{13}C,^{15}N]CTnC in the beginning and the end of the titration are shown in Fig. 3 *a* and *b*, respectively. Each cross-peak corresponds to ^{15}N and ^{1}H resonances of the amide of an individual amino acid. Assignments for some of the peaks are indicated in both spectra. The two spectra are clearly different. These differences were observed during the titration as a gradual shifting of the resonances of the residues affected by TnT-(160–193). The binding occurs with fast exchange kinetics on the NMR time scale. The peaks in each titration point correspond to the weighted average of peptide-free and peptide-bound peaks. This shifting can be seen in Fig. 4, which shows a superimposition of a region of the two-dimensional ^{1}H,^{15}N HSQC NMR spectra of [^{13}C,^{15}N]CTnC during the titration. While some cross-peaks almost do not change, like those for Ala-124 and Leu-137, others are greatly displaced in different directions, as exemplified by the cross-peaks for Glu-159 and Lys-156. The peaks stop moving when the $[\text{TnT-(160–193)}]_{total}/[\text{CTnC}]_{total}$ ratio reaches 1, indicating the binding of only one TnT-(160–193) per CTnC.

Titration of whole TnC with TnT-(160–193) produced similar results for residues in the C-terminal domain. Residues in the N-terminal domain did not move significantly until the C-terminal domain was saturated, and then they began to move. Because the N domains of two TnC molecules can interact, forming a TnC dimer (18), chemical shift changes in the N domain can be caused by breaking of the dimer. Peak displacements (the total chemical shift changes) for each residue were calculated from the chemical shift changes of both nuclei using Equation 1 (9).

$$\Delta\delta_{total} = \sqrt{(\Delta\delta_{15_N})^2 + (\Delta\delta_{1_H})^2} \qquad \text{(Eq. 1)}$$

A comparison of the NMR chemical shift changes for residues in the C domain for both titrations can be seen in Fig. 5. The chemical shift changes for each residue were similar in both titrations, except for the first nine residues in CTnC. This difference is probably caused by the different environments for this region in the two proteins. While these residues are in the middle of the protein in TnC, in CTnC they are the N-terminal residues.

The residues in the C domain that had a chemical shift change greater than 100 Hz at the end of the titration were averaged and normalized in both titrations, and the results were plotted in the binding curves shown in Fig. 6. Five non-overlapping cross-peaks for residues in the N domain that moved more than 40 Hz were also averaged, normalized to the C domain values, and plotted in Fig. 6*a*. The curves were fitted to binding using Equation 2,

$$\text{TnC}+\text{TnT-(160–193)} \leftrightarrows \text{TnC·TnT-(160–193)} \qquad \text{(Eq. 2)}$$

where TnC represents both [^{15}N]TnC and [^{15}N,^{13}C]CTnC. The resulting dissociation constants were 30 ± 6 μM for the C domain of whole TnC and 38 ± 24 μM for CTnC. To calculate the N domain binding curve, TnT-(160–193) concentrations were adjusted at each point for the free TnT-(160–193) concentrations. The dissociation constant for the N domain cannot be accurately determined because the site did not saturate during the titration. It can be seen, however, that it is at least 10 times bigger than for the C domain and that the binding to the N domain is not significant until the C domain is 90% saturated. The curve for the N domain in Fig. 6 was plotted using K_D = 400 μM, the minimum value that fitted the data.

Peak displacements caused by the binding of TnT-(160–193) (shown in Fig. 5) were mapped on the protein surface both for

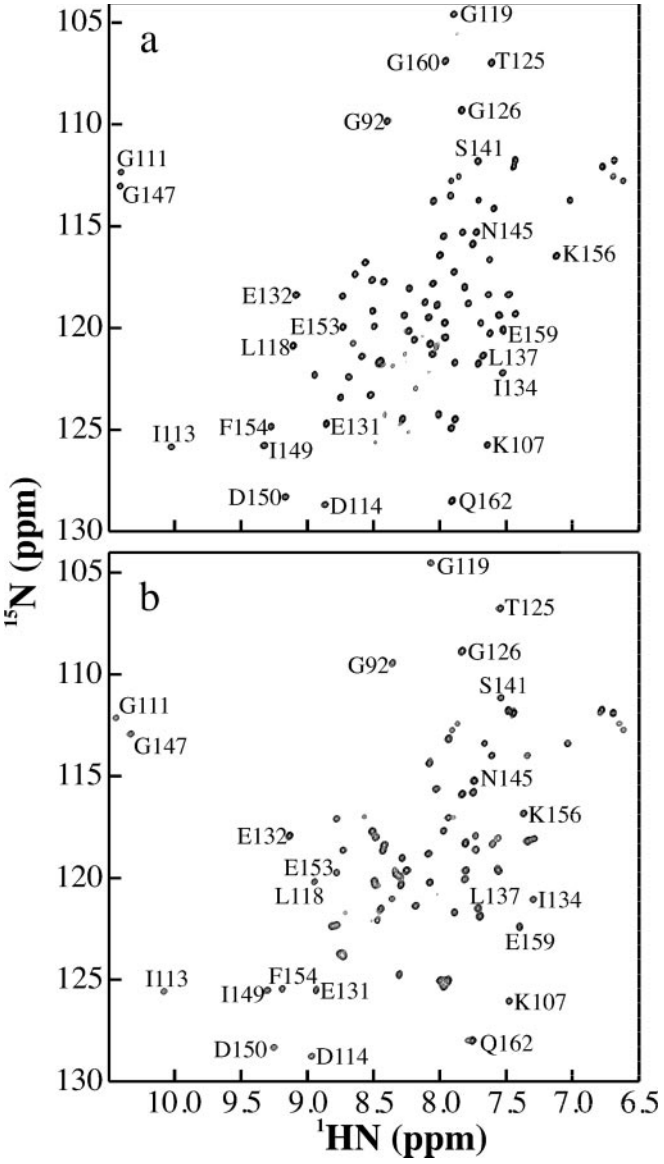

FIG. 3. **Titration of CTnC with TnT-(160–193).** Contour plots of the 600 MHz two-dimensional ^{1}H,^{15}N HSQC NMR spectrum of CTnC. *a*, in the absence of TnT-(160–193); and *b*, saturated with TnT-(160–193). Chemical shift values for ^{15}N and ^{1}H in each amide cross-peak correspond to the *y*- and *x*-axis values. Assignments for some residues are indicated.

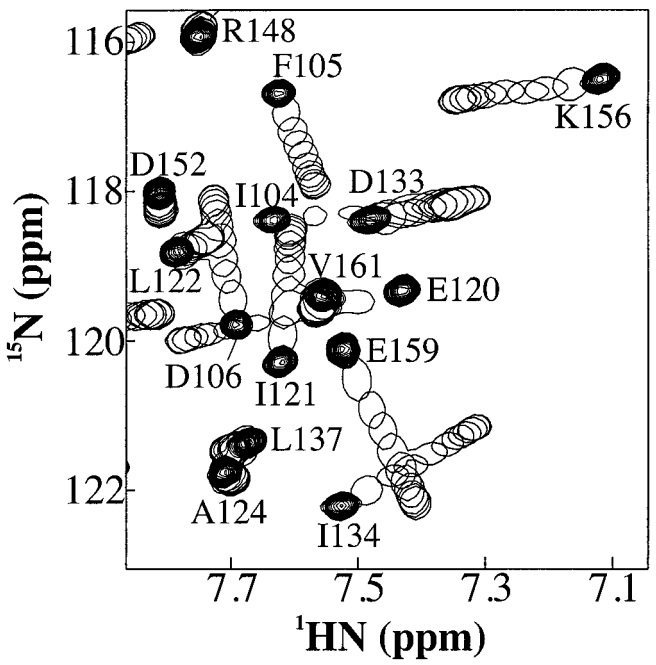

FIG. 4. **Shifting of CTnC amide NMR cross-peaks during titration with TnT-(160–193).** A detail of the two-dimensional ^{1}H,^{15}N HSQC NMR spectrum of CTnC in the absence of TnT-(160–193) is shown in multiple contours, while peaks in the same region of the spectrum after each peptide addition are shown in single contours.

the C domain in the presence of TnI-(1–47) and for the whole TnC in the model of TnC·TnI (Fig. 7). The surface was colored in a gradient according to the degree to which the residues were affected by TnT-(160–193) binding. Regions in *white* correspond to residues whose amide chemical shift, according to Equation 1, did not change by more than 20 Hz during the titration. Residues whose peaks shifted more than 120 Hz were colored in pure *red*. Through this mapping, the TnT-(160–193)-binding site on TnC can be visualized in the protein and in the binary complex model.

DISCUSSION

Among the five peptides covering the whole T2 region in rabbit fast skeletal muscle TnT, two peptides, containing residues 160–193 and 228–260, bind TnC according to non-denaturing gel electrophoresis data. These regions must therefore contain the physiologically important TnC-binding sites in TnT. Any binding too weak to be seen as a band in the gel under the conditions used is not likely to be physiological. These results are in good agreement with previous results from the literature. Most studies showed Ca^{2+}-dependent binding to TnC of larger peptides from the T2 region or the whole T2 containing residues 160–193 (31–34). The smallest of them contained residues 160–210. There is also evidence of binding for peptides containing residues 207–259, 177–231, and 240–260 (31), although the last two peptides did not form complexes that could be detected by electrophoresis (35). The peptide containing residues 177–231 contains half of TnT-(160–193), whereas 207–259 and 240–260 overlap with TnT-(228–260). As in our experiments, these studies showed weaker binding in the absence of Ca^{2+}, even in the presence of Mg^{2+} (31–33). Different studies have suggested that the C domain of TnC adopts different conformations when bound to Ca^{2+} or Mg^{2+} (36, 37).

TnT-(228–260) seems to have a primary binding site on TnC but also binds TnC nonspecifically in increased concentrations. This nonspecific binding can affect affinity measurements and binding site mapping. Preliminary NMR studies showed that the peptide aggregates when in solution, and the complex TnC·TnT-(228–260) precipitates in the NMR tube (data not shown). For these reasons, we centered this work on the characteristics of TnT-(160–193) binding to TnC.

The binding site for TnT-(160–193) is located on the C-terminal domain of TnC. Not only is TnT-(160–193) capable of binding to CTnC, but the same residues are involved in the binding of TnT-(160–193) to the whole protein and to CTnC, showing that the peptide is bound to the same site in both situations. When the C domain is saturated, TnT-(160–193) binds to the N domain of TnC. That binding, however, occurs with much lower affinity (more than 10 times lower) and is likely non-physiological.

The dissociation constant for TnC·TnT-(160–193) binding is 30 ± 6 μM. The affinity between TnC and TnT was previously reported as almost 1000 times stronger (38). This difference can be caused by different conditions or different measuring methods, but most probably because we used a small peptide

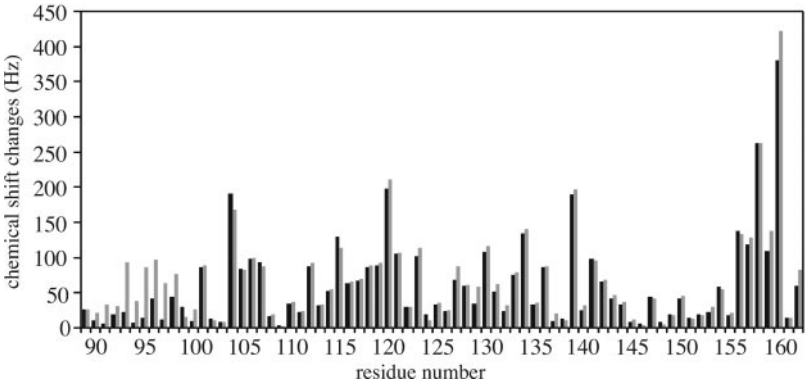

FIG. 5. **Backbone amide NMR chemical shift changes in TnC (*black*) and CTnC (*gray*) upon TnT-(160–193) binding.** The total chemical shift change (δ_{total}) for each residue was calculated from Equation 1. The $[TnT\text{-}(160–193)]_{total}/[CTnC]_{total}$ ratio was equal to 1.18, and the $[TnT\text{-}(160–193)]_{total}/[TnC]_{total}$ ratio was equal to 1.14.

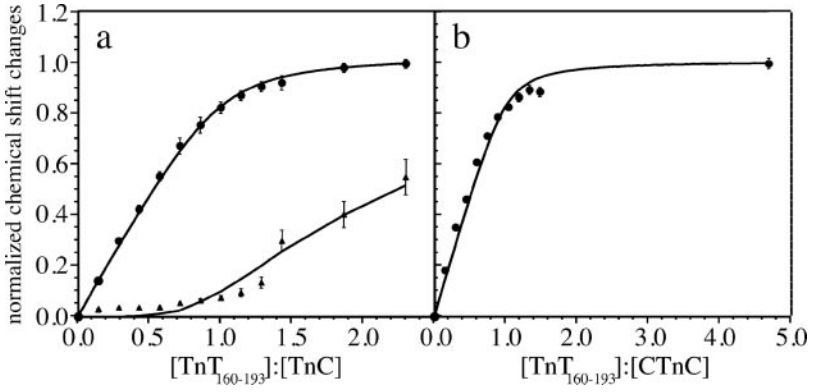

FIG. 6. **TnT-(160–193) binding curves to TnC and CTnC, plotted from NMR chemical shift changes in the amide cross-peak in the $^{1}H,^{15}N$ HSQC NMR spectra against total TnT-(160–193)/TnC ratio.** *a*, binding curves of TnT-(160–193) to [^{15}N]TnC. ●, residues in the C domain (K_D = 30.4 ± 6.0 μM); ▲, residues in the N domain ($K_D \approx$ 400 μM). The data for both curves were normalized using the maximum chemical shift changes for the C domain. *b*, binding curve of TnT-(160–193) to [^{15}N,^{13}C]CTnC (K_D = 38 ± 24 μM). The *error bars* represent the normalized standard deviation for each point. The dissociation constant for the C domain in both titrations was calculated by fitting the data to the binding equation (Eq. 2) with the program xcrvfit. The dissociation constant for the N domain cannot be accurately calculated because the site did not saturate during the experiment. An approximate curve was plotted using K_D = 400 μM. Residues 8, 35, 64, 69, and 85 were used for the N domain plot, while residues 101, 104, 107, 112, 118 to 121, 123, 130, 134, 139, 141, 156, 157, and 159 were used in the C domain curve fitting for [^{15}N]TnC titration. Residues 93, 95, 96, 101, 104, 106, 107, 112, 115, 118 to 121, 123, 130, 134, 139, 141, 156, and 159 were used in the curve fitting for [^{15}N,^{13}C]CTnC.

whereas the previous measurement was made using the whole protein. The presence of residues 228–206 from TnT probably strengthens the interaction. The difference between the affinity of TnT-(160–193) for CTnC and TnC is not statistically significant. On the other hand, the increased flexibility of the N-terminal residues of CTnC may weaken the binding to TnC. The CTnC titration did not have enough points to obtain a smaller error in the curve fitting.

The binding data for the N domain in Fig. 6 has a slightly more sigmoid shape than the expected binding curve. This could be the result of breaking any partial dimerization of TnC. TnC dimerizes through the N domain (18), and the observed chemical shift changes for the N domain are the combined effect of TnT-(160–193) binding and breaking of the dimer. TnT-(160–193) binds to the N domain of TnC in the monomeric state, and both reactions contribute to the binding curve.

The site was mapped on the surface of TnC in one of the two recently published models for the TnC·TnI binary complex "model L" (15) (Fig. 7). The binding site involves hydrophobic, negative, and positive residues, mostly between the EF hand sites III and IV. Residues 104–107, in the beginning of site III, form the first binding cluster. One side of both helices F and G is also involved, and residues 156–160, close to the C-terminal of the protein, complete the binding site for TnT-(160–193). TnC orientation in Fig. 7 was chosen to show the binding site. The surface not seen on the figure is mostly white and not affected by TnT-(160–193). Chemical shift changes in the N domain were not mapped on the protein surface because they possibly reflect the dimerization state of TnC.

The region containing residues 160–193 in TnT involved in TnC binding is immediately N-terminal from the TnI-binding region. Residues 198–251 of TnT contain a hydrophobic heptad repeat, typical of a coiled-coil structure, that has been proposed to interact with residues 57–106 of TnI, which also contain a hydrophobic heptad repeat (39). A TnT fragment containing residues 177–231 of TnT bind to TnI (39), while a chicken TnT mutant missing residues 216–263 (40) and a bovine TnT mutant missing residues 203–214 (41) cannot bind TnI. These regions correspond to residues 211–260 and 205–216 in rabbit TnT_{2f}, respectively. Residues 224–228 were also shown to be critical for TnI binding (33).

Since regions of TnT responsible for TnC and TnI binding are located side by side, it is expected that the corresponding regions of TnC and TnI that interact with TnT would be closely located in the troponin complex. In the model in Fig. 7, the region containing the hydrophobic heptad repeat in TnI (residues 57–106) corresponds mostly to the α-helix (seen in *blue* to the *left* of the C domain of TnC), which does not interact with TnC in the complex. It is, however, close enough to the mapped TnT-binding site on TnC (colored in *red*) to suggest that these regions could interact with consecutive regions in TnT.

The non-denaturing gel electrophoresis data (Fig. 1*c*) showed that TnT-(160–193) and TnI-(1–40) can bind to TnC at the same time. The region of TnI corresponding to TnI-(1–40) is shown in *green* in Fig. 7. Even though both peptides bind to same region of TnC, they do not interact with the same residues and would not compete for TnC binding. NMR chemical shift changes mapping the TnI-(1–40)-binding site on CTnC

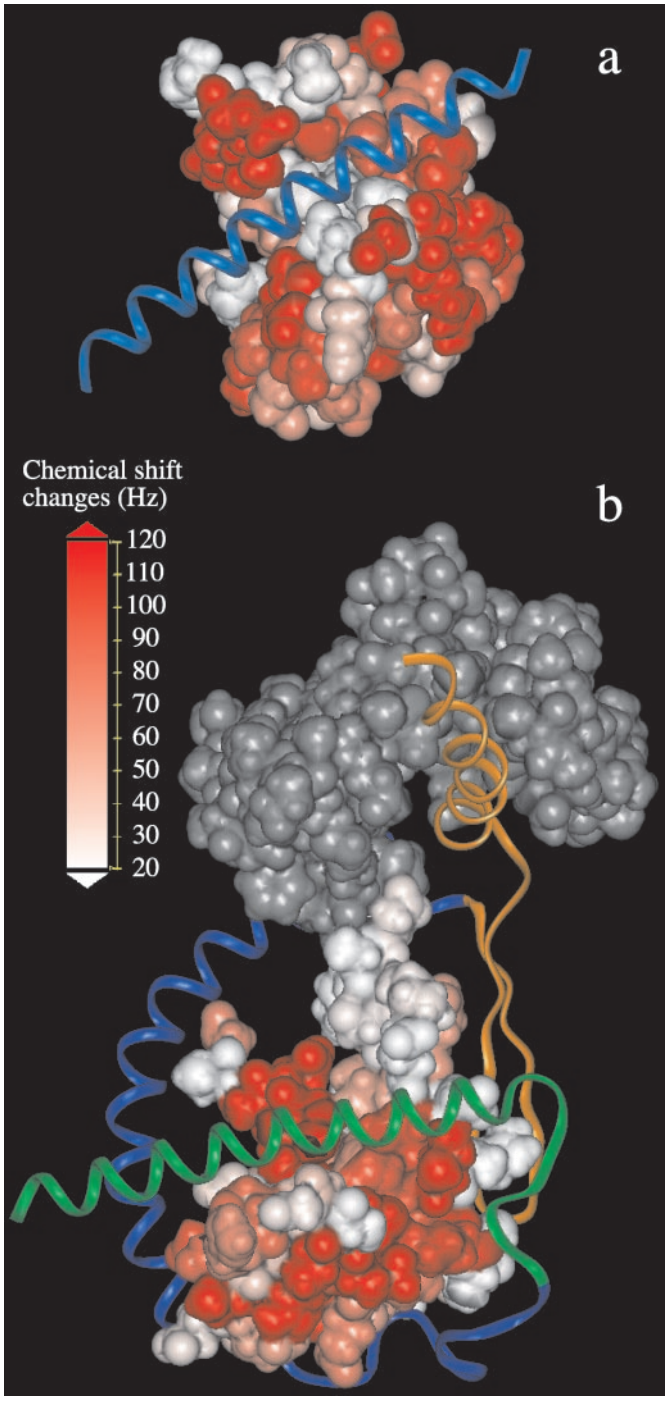

FIG. 7. **Molecular surface mapping of the TnT-(160–193) binding site in the C domain of TnC.** The TnT-(160–193) binding site is shown in TnC·TnI complexes. TnC is shown as a *surface*, while TnI is shown in *ribbon* representation. *a*, mapping of TnT-(160–193) binding to CTnC, shown on CTnC crystal structure complexed to TnI-(1–47) (11); *b*, mapping of TnT-(160–193) binding to whole TnC, shown on the model L of the binary complex TnC·TnI (15). The surfaces were colored according to the gradient on the figure, going from *white*, for the residues whose cross-peaks moved less than 20 Hz, to *red*, for the residues whose cross-peaks moved more than 120 Hz. In *b*, the region of TnI corresponding to the peptide TnI-(1–40) is colored in *green*, while the region corresponding to TnI-(96–139) is colored in *orange*.

showed that the binding affects the residues in the hydrophobic pocket of CTnC (14), while TnT-(160–193) affects mostly the external surface of helices F and G in the region exposed to the solvent.

TnI-(96–139) (Fig. 7, *orange region*) and TnI-(56–115) compete with TnT-(160–193) binding to TnC, indicating that they share at least part of the binding site on TnC. TnI-(96–139) contains the inhibitory peptide (residues 96–115), shown as the *orange* β-hairpin to the *right* of TnC in Fig. 7, and an α-helical region (residues 116–139) that binds to the N domain of TnC (9). The inhibitory peptide is the only common region between the two peptides, and must, therefore, be the region that competes with TnT-(160–193). The model for the TnC·TnI binary complex shown in Fig. 7 does not account for that competition.

We suggest that the binding site for the inhibitory peptide on TnC overlaps the TnT-binding site, at least partially. The inhibitory peptide is located close to TnT in the troponin complex, and the presence of TnT can protect the inhibitory region from chymotryptic digestion (42). As for TnT-(160–193), TnI-(96–115) has both electrostatic and hydrophobic interactions with CTnC, while TnI-(1–40) has mostly hydrophobic interactions (14). TnT-(160–193) and TnI-(96–115) may share some of the electrostatic contacts and therefore compete for TnC.

It is interesting to observe that while TnI-(96–115) competes with TnI-(1–40) and presumably with TnT-(160–193), TnI-(1–40) and TnT-(160–193) do not compete. The binding site for the inhibitory peptide probably shares different residues with TnI-(1–40)- and TnT-(160–193)-binding sites, so that the last two sites either do not overlap or the overlapping region is so small that it does not significantly affect the binding.

Thus our results support much of model L from Tung *et al.* (15), except for the exact position of the inhibitory peptide. Model R is not compatible with our results. The position of TnI residues 3–33 in model R, overlapping the mapped TnT-(160–193)-binding site, would cause competition between TnI-(1–40) and TnT-(160–193). We suggest that model L is probably closer to the actual structure of the binary TnC·TnI complex. This is the first time that a TnT-binding site has been mapped on TnC. When combined with the information available on TnI binding to TnC, the mapping offers insights into how the three components come together in the structure of troponin tertiary complex.

Acknowledgments—We thank Robert Boyko for developing xcrvfit software, David Corson for expressing and purifying TnC and its domains, and Gerry McQuaid for maintenance of the NMR spectrometers. We thank Pascal Mercier and Dr. Leo Spyracopoulos for advice and help during this work.

REFERENCES

1. Zot, A. S., and Potter, J. D. (1987) *Annu. Rev. Biophys. Biophys. Chem.* **16,** 535–559
2. Farah, C. S., and Reinach, F. C. (1995) *FASEB J.* **9,** 755–767
3. Tobacman, L. S. (1996) *Annu. Rev. Physiol.* **58,** 447–481
4. Herzberg, O., and James, M. N. G. (1988) *J. Mol. Biol.* **203,** 761–779
5. Satyshur, K. A., Rao, S. T., Pyzalska, D., Drendel, W., Greaser, M., and Sundaralingam, M. (1988) *J. Biol. Chem.* **263,** 1628–1647
6. Houdusse, A., Love, M. L., Dominguez, R., Grabarek, Z., and Cohen, C. (1997) *Structure* **5,** 1695–1711
7. Slupsky, C. M., and Sykes, B. D. (1995) *Biochemistry* **34,** 15953–15964
8. Campbell, A. P., and Sykes, B. D. (1991) *J. Mol. Biol.* **222,** 405–421
9. McKay, R. T., Tripet, B. P., Hodges, R. S., and Sykes, B. D. (1997) *J. Biol. Chem.* **272,** 28494–28500
10. McKay, R. T., Pearlstone, J. R., Corson, D. C., Gagné, S. M., Smillie, L. B., and Sykes, B. D. (1998) *Biochemistry* **37,** 12419–12430
11. Vassylyev, D. G., Takeda, S., Wakatsuki, S., Maeda, K., and Maeda, Y. (1998) *Proc. Natl. Acad. Sci. U. S. A.* **95,** 4847–4852
12. Hernández, G., Blumenthal, D. K., Kennedy, M. A., Unkefer, C. J., and Trewhella, J. (1999) *Biochemistry* **38,** 6911–6917
13. Li, M. X., Spyracopoulos, L., and Sykes, B. D. (1999) *Biochemistry* **38,** 8289–8298
14. Mercier, P., Li, M. X., and Sykes, B. D. (2000) *Biochemistry* **39,** 2902–2911
15. Tung, C.-S., Wall, M. E., Gallagher, S. C., and Trewhella, J. (2000) *Protein Sci.* **9,** 1312–1326
16. Perry, S. V. (1998) *J. Muscle Res. Cell Motil.* **19,** 575–602
17. Potter, J. D., Sheng, Z., Pan, B.-S., and Zhao, J. (1995) *J. Biol. Chem.* **270,** 2557–2562
18. Slupsky, C. M., Kay, C. M., Reinach, F. C., Smillie, L. B., and Sykes, B. D. (1995) *Biochemistry* **34,** 7365–7375
19. Gagné, S. M., Tsuda, S., Li, M. X., Chandra, M., Smillie, L. B., and Sykes, B. D. (1994) *Protein Sci.* **3,** 1961–1974
20. Wagschal, K., Tripet, B., and Hodges, R. S. (1999) *J. Mol. Biol.* **285,** 785–803
21. Tripet, B. P., Van Eyk, J. E., and Hodges, R. S. (1997) *J. Mol. Biol.* **271,** 728–750

22. Ngai, S.-M., and Hodges, R. S. (1992) *J. Biol. Chem.* **267,** 15715–15720
23. Sereda, T. J., Mant, C. T., Quinn, A. M., and Hodges, R. S. (1993) *J. Chromatogr.* **646,** 17–30
24. Briggs, M. M., and Schachat, F. (1989) *J. Mol. Biol.* **206,** 245–249
25. Katayama, E., and Nozaki, S. (1982) *J. Biochem.* (*Tokyo*) **91,** 1449–1452
26. Farah, C. S., Miyamoto, C. A., Ramos, C. H. I., Silva, A. C. R., Quaggio, R. B., Fujimori, K., Smillie, L. B., and Reinach, F. C. (1994) *J. Biol. Chem.* **269,** 5230–5240
27. Kay, L. E., Keifer, P., and Saarinen, T. (1992) *J. Am. Chem. Soc.* **114,** 10663–10665
28. Zhang, O., Kay, L. E., Olivier, J. P., and Forman-Kay, J. D. (1994) *J. Biomol. NMR* **4,** 845–858
29. Delaglio, F., Grzesiek, S., Vuister, G. W., Zhu, G., Pfeifer, J., and Bax, A. (1995) *J. Biomol. NMR* **6,** 277–293
30. Johnson, B. A., and Blevins, R. A. (1994) *J. Biomol. NMR* **4,** 603–614
31. Pearlstone, J. R., and Smillie, L. B. (1978) *Can. J. Biochem.* **56,** 521–527
32. Pearlstone, J. R., and Smillie, L. B. (1982) *J. Biol. Chem.* **257,** 10587–10592
33. Tanokura, M., Tawada, Y., Ono, A., and Ohtsuki, I. (1983) *J. Biochem.* (*Tokyo*) **93,** 331–337
34. Raggi, A., Grand, R. J. A., Moir, A. J. G., and Perry, S. V. (1989) *Biochim. Biophys. Acta* **997,** 135–143
35. Jackson, P., Amphlett, G. W., and Perry, S. V. (1975) *Biochem. J.* **151,** 85–97
36. Trigo-Gonzalez, G., Racher, K., Burtnick, L., and Borgford, T. (1992) *Biochemistry* **31,** 7009–7015
37. Finley, N., Dvoretsky, A., and Rosevear, P. (2000) *J. Mol. Cell. Cardiol.* **32,** 1439–1446
38. Ingraham, R. H., and Swenson, C. A. (1984) *J. Biol. Chem.* **259,** 9544–9548
39. Pearlstone, J. R., and Smillie, L. B. (1985) *Can. J. Biochem.* **63,** 212–218
40. Malnic, B., Farah, C. S., and Reinach, F. C. (1998) *J. Biol. Chem.* **273,** 10594–10601
41. Stefancsik, R., Jha, P. K., and Sarkar, S. (1998) *Proc. Natl. Acad. Sci. U. S. A.* **95,** 957–962
42. Tao, T., Gong, B.-J., Grabarek, Z., and Gergely, J. (1999) *Biochim. Biophys. Acta* **1450,** 423–433